PI(3,4)P2 plays critical roles in the regulation of focal adhesion dynamics of MDA-MB-231 breast cancer cells

Fukumoto, Miki

Ijuin, Takeshi

Takenawa, Tadaomi

(Citation)
Cancer Science,108(5):941-951

(Issue Date)
2017-05

(Resource Type)
journal article

(Version)
Version of Record

(URL)
https://hdl.handle.net/20.500.14094/90004039

Cancer Science
Japanese Cancer Association JCA
Open Access

PI(3,4)P_2 plays critical roles in the regulation of focal adhesion dynamics of MDA-MB-231 breast cancer cells

Miki Fukumoto,[1] Takeshi Ijuin[2] and Tadaomi Takenawa[3]

[1]The Integrated Center for Mass Spectrometry, Kobe University Graduate School of Medicine, Kobe; Divisions of [2]Biochemistry, Kobe University Graduate School of Medicine, Kobe; [3]Molecular and Cell Biology, Kobe University Graduate School of Medicine, Kobe, Japan

Key words
Cell invasion, focal adhesion, Lpd, PI(3,4)P_2, SHIP2

Correspondence
Takeshi Ijuin, Division of Biochemistry, Kobe University Graduate School of Medicine, 7-5-1 Kusunoki, Chu-o, Kobe, 650-0017, Japan.
Tel: +81-78-382-5429; Fax: +81-78-382-5439;
E-mail: tijuin@med.kobe-u.ac.jp

Funding Information
This work was supported by grants to T. I. from the Japan Society for the Promotion of Science (JSPS; Kakenhi grant number 16K08585).

Received October 20, 2016; Revised February 17, 2017; Accepted February 22, 2017

Cancer Sci **108** (2017) 941–951

doi: 10.1111/cas.13215

Phosphoinositides play pivotal roles in the regulation of cancer cell phenotypes. Among them, phosphatidylinositol 3,4-bisphosphate (PI(3,4)P_2) localizes to the invadopodia, and positively regulates tumor cell invasion. In this study, we examined the effect of PI(3,4)P_2 on focal adhesion dynamics in MDA-MB-231 basal breast cancer cells. Knockdown of SHIP2, a phosphatidylinositol 3,4,5-trisphosphatase (PIP_3) 5-phosphatase that generates PI(3,4)P_2, in MDA-MB-231 breast cancer cells, induced the development of focal adhesions and cell spreading, leading to the suppression of invasion. In contrast, knockdown of PTEN, a 3-phosphatase that de-phosphorylates PIP_3 and PI(3,4)P_2, induced cell shrinkage and increased cell invasion. Interestingly, additional knockdown of SHIP2 rescued these phenotypes. Overexpression of the TAPP1 PH domain, which binds to PI(3,4)P_2, and knockdown of Lpd, a downstream effector of PI(3,4)P_2, resulted in similar phenotypes to those induced by SHIP2 knockdown. Taken together, our results suggest that inhibition of PI(3,4)P_2 generation and/or downstream signaling could be useful for inhibiting breast cancer metastasis.

Breast cancer metastasis is one of the major causes of cancer-related mortality in women worldwide. Metastasis is a multistep process: after cell spreading, cancer cells form lamellipodia and migrate through the assembly of branched F-actin networks. This cytoskeletal rearrangement is mediated by actin-regulatory proteins including Rac1, WAVEs, and Mena/Ena/VASP proteins. Mena is frequently upregulated in breast cancer cells and promotes cell invasion. Lamellipodin (Lpd, also referred to as Raph1) localizes to lamellipodia and recruits Mena/Ena/VASP to membrane protrusions.[1] Lpd was shown to regulate random motility in breast cancer cells and is required for lamellipodia formation.[2,3]

PI3-kinase (PI3K) signaling has critical roles in cell proliferation, survival, and motility. PIP_3, generated from PI(4,5)P_2 through PI3K activity, is an important secondary messenger involved in the activation of Akt. A high proportion of breast cancer cells acquire the ability to activate and sustain PI3K/Akt signaling, which contributes to therapeutic resistance. More than 70% of breast cancers have alterations in at least one component of the PI3K/Akt pathway, including PIK3CA, PTEN, and Akt.[4–6] Among them, *PIK3CA*, the gene that encodes the catalytic subunit of Class 1 PI3K, is mutated and activated in breast cancers.[7,8] These mutations, most frequently observed in estrogen and/or progesterone receptor-positive and HER2-positive breast tumors, but rarely identified in triple-negative tumors,[9] lead to the activation of PI3K/Akt signaling, resulting in the initiation of breast cancer. PTEN, a tumor suppressor that hydrolyzes PIP_3 to PI(4,5)P_2 suppresses PI3K/Akt signaling.[10,11] Although PTEN mutations are less frequent, loss of heterozygosity at the *PTEN* locus frequently occurs in breast cancer.[9,12] PTEN loss is observed in 30–40% of sporadic cases of breast cancer that are associated with hyperactivation of PI3K/Akt signaling, and results in the accumulation of PIP_3[13,14] and tumor progression.[15,16] In addition, the phosphoinositide 4-phosphatase, INPP4B, which hydrolyzes PI(3,4)P_2 to PI(3)P, inhibits PI3K/Akt signaling, and was identified as a tumor suppressor in breast cancer.[17,18] In 84% of basal-like breast cancers, loss of INPP4B expression occurs[17] and INPP4B loss-of-heterogeneity frequently occurs in BRCA1-mutant and triple-negative basal-like breast cancers.[18] INPP4B knockdown was shown to induce Akt activation and anchorage-independent growth.[18] In addition, loss of heterogeneity at the *INPP4B* locus was found in the majority of estrogen receptor-negative basal-like breast cancers.[17]

Recent studies identified that a number of phosphoinositide 5-phosphatases that hydrolyze PIP_3 to PI(3,4)P_2, such as SHIP, SKIP, and PIPP, were also found to act as PI3K/Akt signal terminators. The expression of SKIP (also referred to as INPP5K) can be altered in brain cancers.[19–21] In PTEN-null glioblastoma cells, SKIP overexpression inhibits cell migration through regulation of the actin cytoskeleton.[22] PIPP (INPP5J) is frequently inactivated in triple-negative breast cancers, and functions as a tumor suppressor.[23] Its inactivation promotes

tumor growth and suppresses metastasis.[23] The SH2 domain-containing inositol 5-phosphatase SHIP2, also referred to as INPPL1, which dephosphorylates PIP_3 and $PI(4,5)P_2$ to generate $PI(3,4)P_2$ and PI(4)P, respectively, has a negative effect on PI3K/Akt signaling.[24,25] SHIP2 knockout mice show mild insulin hypersensitivity and resistance to high fat diet-induced obesity.[26] This protein is overexpressed in human breast cancers, and correlates with shorter survival.[27] SHIP2 localizes to the focal contacts and lamellipodia,[27,28] and it inhibits cell migration in PTEN-null 1321 N1 glioblastoma cells through de-phosphorylation of $PI(4,5)P_2$.[29,30] In contrast, a number of studies have suggested that SHIP2 is often amplified in human cancer cells,[31–33] whereas the tumor suppressors PTEN and INPP4B are often mutated or deleted, which leads to sustained activation of PIP_3-dependent Akt signaling in these cells. However, it is not clear how amplification of SHIP2 is involved in the malignancy of cancer cells, though this event is expected to lead to decreased PIP_3 levels.

Increasing evidence suggests that $PI(3,4)P_2$, which is generated from PIP_3, not only induces the activation of Akt, but can act independently to regulate processes such as of membrane ruffle formation,[34] podosome formation,[27] lamellipodia formation,[1] and lamellipodia maturation.[35] Recent study showed that $PI(3,4)P_2$ depletion impairs motility during B cell chemotaxis, and that Lpd, whose PH domain specifically binds to $PI(3,4)P_2$, co-localizes with $PI(3,4)P_2$ to mediate directional migration.[36] Thus, $PI(3,4)P_2$ is an important signaling molecule that is involved in regulating cytoskeletal rearrangements at the plasma membrane.[37] Other studies have demonstrated the role of Lpd in the actin cytoskeletal network. Lpd and Ena/VASP were found to interact with the WAVE regulatory complex,[3,38] membrane-bound Lpd directly binds to filamentous actin and recruits Ena/VASP, and WAVE activities the lamellipodial actin network.[39]

Focal adhesions (FAs) are macromolecular assemblies that sense extracellular stimuli and signaling complexes that play central roles in cell migration.[40] Upon mechanical tension, some grow into larger and stable FAs and recruit various proteins including zyxin (ZYX) through a process known as FA maturation to modulate integrin signaling for cell migration.[41] Lpd and several focal adhesion proteins, including focal adhesion kinase (FAK), the adapter proteins p130Cas (Cas), and paxillin (PAX), play a role in transducing ECM stiffness into intracellular stiffness.[42] The information encoded by ECM stiffness is transduced into intracellular stiffness by integrins, the transmembrane adhesion receptors for ECM proteins, focal adhesion proteins, and the actin cytoskeleton. Vinculin, a focal adhesion protein that binds to $PI(4,5)P_2$, has been implicated in the stiffness-sensing event.[43] However, it is still unclear whether $PI(3,4)P_2$ and its effector protein Lpd regulate focal adhesion dynamics and migration in breast cancer cells.

We hypothesized that $PI(3,4)P_2$ has a pivotal role in focal adhesion dynamics and lamellipodia formation, leading to increased motility and invasion in cancer cells. In this study, we examined the effect of SHIP2 and/or PTEN knockdown on the dynamic regulation of focal adhesion formation and the invasion of *PTEN*-positive and *INPP4B*-null MDA-MB-231 basal breast cancer cells, and found that knockdown of SHIP2 decreased $PI(3,4)P_2$ levels, which in turn induced the development of FA and the suppression of invasion. Our results indicate that the $PI(3,4)P_2$-Lpd dependent pathway, but not the $PI(4,5)P_2$-FAK signaling pathway, controls focal adhesion dynamics in breast cancer cells.

Materials and methods

Reagents and antibodies. The anti-phospho-FAK (Tyr-397) antibody (Catalog No. 44-624G) was purchased from Life Technologies (Carlsbad, CA, USA). Anti-FAK antibody (Catalog No. 610087) was purchased from BD Transduction Laboratories (San Jose, CA. USA). Anti-pan Akt (Catalog No. 5084) and anti-phospho-Akt (Ser-473, Catalog No. 4060) antibodies were purchased from Cell Signaling Technology (Danvers, MA, USA). The anti-zyxin (ZYX) (Catalog No. HPA004835) and anti-vinculin (VCL) (Catalog No. V9131) antibodies were purchased from Sigma-Aldrich (St. Louis, MO, USA). The anti-SHIP2 (Catalog No. 2839) and anti-phospho-paxillin (PAX) (Tyr-118, Catalog No. 2541) antibodies were purchased from Cell Signaling Technology. The anti-paxillin antibody (Catalog No. 610051) was from BD Biosciences (San Jose, CA. USA). The anti-actin antibody (Catalog No. MAB1501) was purchased from EMD Millipore (Billerica, MA, USA). LY294002 and wortmannin were purchased from Merck Millipore (Darmstadt, Germany).

Cell culture. The human breast cancer MDA-MB-231 cell line was purchased from the American Type Culture Collection (ATCC, Manassas, VA, USA). Cells were cultured in Dulbecco's modified Eagle's medium (DMEM, Wako, Osaka, Japan) supplemented with 10% fetal bovine serum (FBS), 4 mM L-glutamine, streptomycin, and penicillin.

Plasmids and transfection. Full-length human SHIP2 cDNA were obtained by reverse transcription (RT)-polymerase chain reaction (PCR) using total RNA isolated from MDA-MB-231 cells as a template. cDNA was cloned into pEGFP-C1 vector (Takara bio, Otsu, Japan). Furthermore, cDNA encoding TAPP1 PH, FAPP1 PH, PLCδ1 PH, and Grp1 PH were isolated as described previously.[44]

RNA interference (RNAi). The following stealth siRNA species (Life Technologies) targeting human SHIP2, PTEN, and Lpd were used for RNAi experiments. The targeted sequences of the Stealth siRNA species used in this study are as follows: control, Stealth RNAi siRNA negative control med GC (Catalog No. 12935-300), SHIP2 #1, 5′- CAGGAGAUCCUGAACU ACAUCAGCA-3′, SHIP2 #2, 5′-GAGGUUGGAGUUACCUC CCAGUUCA-3′, PTEN, 5′-CCAAUGGCUAAGUGAAGAU GACAAU-3′, Lpd #1, 5′-CCAGCUGGAUCAUGUCAACGU UUAU-3′, and Lpd #2, 5′-GCAAAGUAUGGGAAGCAGCU CUAUA-3′. siRNA was transfected into MDA-MB-231 cells using Lipofectamine RNAiMAX reagent (Life Technologies) according to the manufacturer's protocol.

Immunofluorescence microscopy. Cells were transfected with plasmids or siRNA for 24–48 h and then re-plated on fibronectin (FN)-coated coverslips. Cells were cultured for 24 h, and then fixed with 4% paraformaldehyde for 10 min at room temperature, which was followed by permeabilization with phosphate-buffered saline (PBS) containing 0.2% Triton X-100 for 5 min. Coverslips were washed twice with PBS and then incubated with primary antibody for 1 h at room temperature. Alexa Fluor 568-conjugated anti-rabbit IgG or anti-mouse antibodies (Life Technologies) were used as secondary antibodies. The coverslips were mounted with PermaFluor Aqueous Mounting Medium (Thermo Scientific, Waltham, MA, USA) and analyzed using a FluoView 1000-D confocal microscope (Olympus, Tokyo, Japan).

Western blotting. MDA-MB-231 cells cultured in FN-coated dishes were lysed with Laemmli sample buffer, briefly sonicated, and boiled at 95°C for 5 min. Western blotting was performed by standard procedures with detection using alkaline

phosphatase-conjugated secondary antibodies (Promega, Madison, MI, USA).

Quantification of focal adhesions and cell area. The number of focal adhesions was calculated as follows. Cells were immunostained with anti-PAX or anti-VCL antibody. The number of PAX- or VCL-positive plaques per cell was counted using ImageJ software (National Institute of Health, Bethesda, MD, USA). Eighty cells were analyzed for each experiment. For the quantification of cell area, cells were immunostained with rhodamine- or Alexa Fluor 647-conjugated phalloidin and were imaged by confocal microscopy. Eighty cells were used to quantify cell area.

Matrigel invasion assay. The invasion assay was performed as previously described. MDA-MB-231 cells were seeded in the upper compartment of a BD Biocoat Matrigel Invasion Chamber (BD Biosciences) and incubated with DMEM containing 10% FBS in the lower well and serum-deprived medium in the top chamber. After 22 h, the cells were fixed with 3.7% formaldehyde in PBS for 30 min. Cells were washed with PBS and cells on the undersurface of the filter were observed by confocal microscopy.

Statistical analysis. For multiple comparisons, *P*-values were generated by one-way analysis of variance using the Student-Newman-Keuls multiple comparison tests. For two group analysis, *P*-values were calculated by Student's *t*-test.

Quantification of phosphoinositides. Plasma membrane phosphoinositides were quantified as follows. To measure PI(3,4)P_2, PI(4,5)P_2, and PIP_3 levels, the laser intensity of EGFP-TAPP1 PH, -PLCδ1 PH, and –GRP1 PH, respectively, were analyzed using the Trainable Weka Segmentation plugin with Image J software.

Results

SHIP2 knockdown increases the number of focal adhesions and cell area. Focal adhesions that connect the actin cytoskeleton with the extracellular matrix and focal adhesion-associated proteins such as Akt, FAK, and PAX, regulate cell invasion, metastasis, and migration.[45–47] These proteins are localized to focal adhesions and are phosphorylated upon focal adhesion development.[47–49] We examined the effect of SHIP2 silencing in MDA-MB-231 breast cancer cells on the expression and activation of Akt, FAK, and PAX. SHIP2 knockdown increased the phosphorylation of PAX at Tyr-118, which is involved in mature focal adhesion formation (Fig. 1a), without affecting phosphorylation of FAK at Tyr-397, and Akt at Ser-473. Since Akt phosphorylation is dependent on PIP_3, these results imply that SHIP2 knockdown increases PIP_3 levels by a very small amount. Next, the effect of SHIP2 knockdown on focal adhesion formation was examined. MDA-MB-231 cells exhibited an elongated shape with polarized membranes, reflecting a highly invasive phenotype. The number of VCL- and ZYX- positive focal adhesions increased after SHIP2 knockdown (Fig. 1b,c). In these cells, stress fibers formed and the cell area also increased (Fig. 1b,d).

SHIP2 alters PI(3,4)P_2 at focal contacts. To examine whether SHIP2 hydrolyzes PIP_3 at focal contacts, GFP-SHIP2 was expressed in MDA-MB-231 cells. This protein was localized

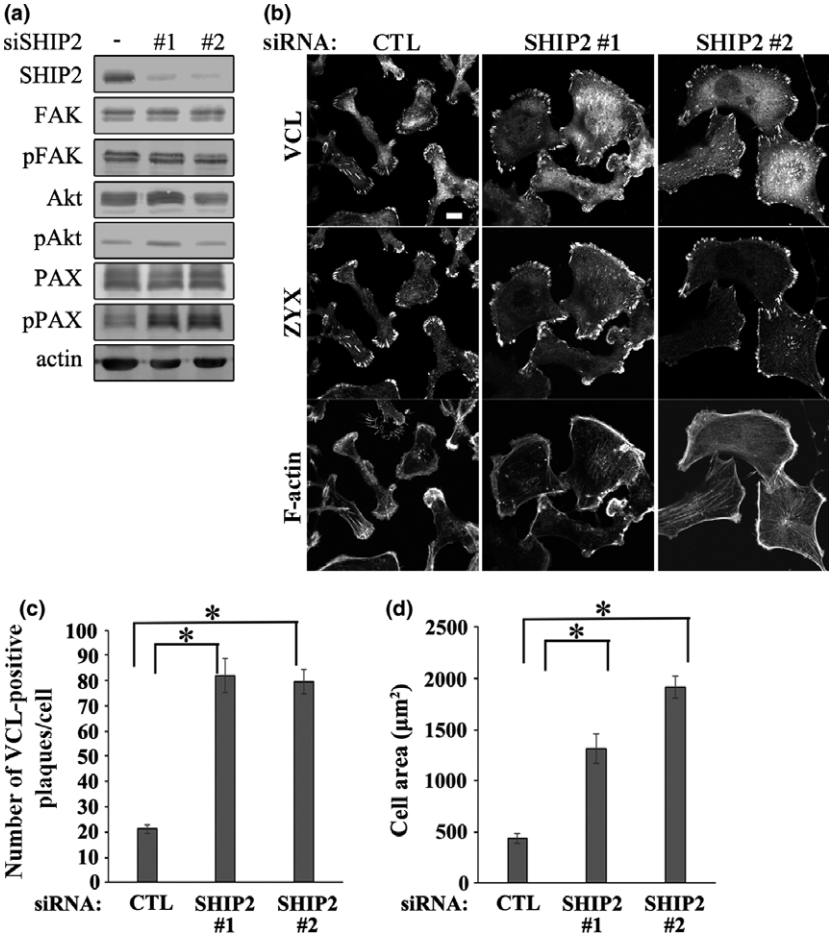

Fig. 1. Effect of SHIP2 knockdown on focal adhesion formation and cell morphology in MDA-MB-231 cells. (a) Lysates from control (–) or SHIP2 siRNA-transfected MDA-MB-231 cells were subjected to western blot analysis using antibodies against SHIP2, FAK, phospho-FAK, Akt, phospho-Akt (Ser-473), PAX, phospho-PAX, and actin. (b) MDA-MB-231 cells transfected with the indicated antibodies were stained with vinculin (VCL) and zyxin (ZYX) antibodies. F-actin was visualized with Alexa Fluor 647 labeled-phalloidin. Scale bar = 10 μm. (c) Quantification of focal adhesion number per cell from (b). (d) Measurement of cell area of cells from (b). All data represent the mean ± SD of 18 cells for the control, 16 cells for siSHIP2 #1, and 16 cells for siSHIP2 #2. *$P < 0.05$.

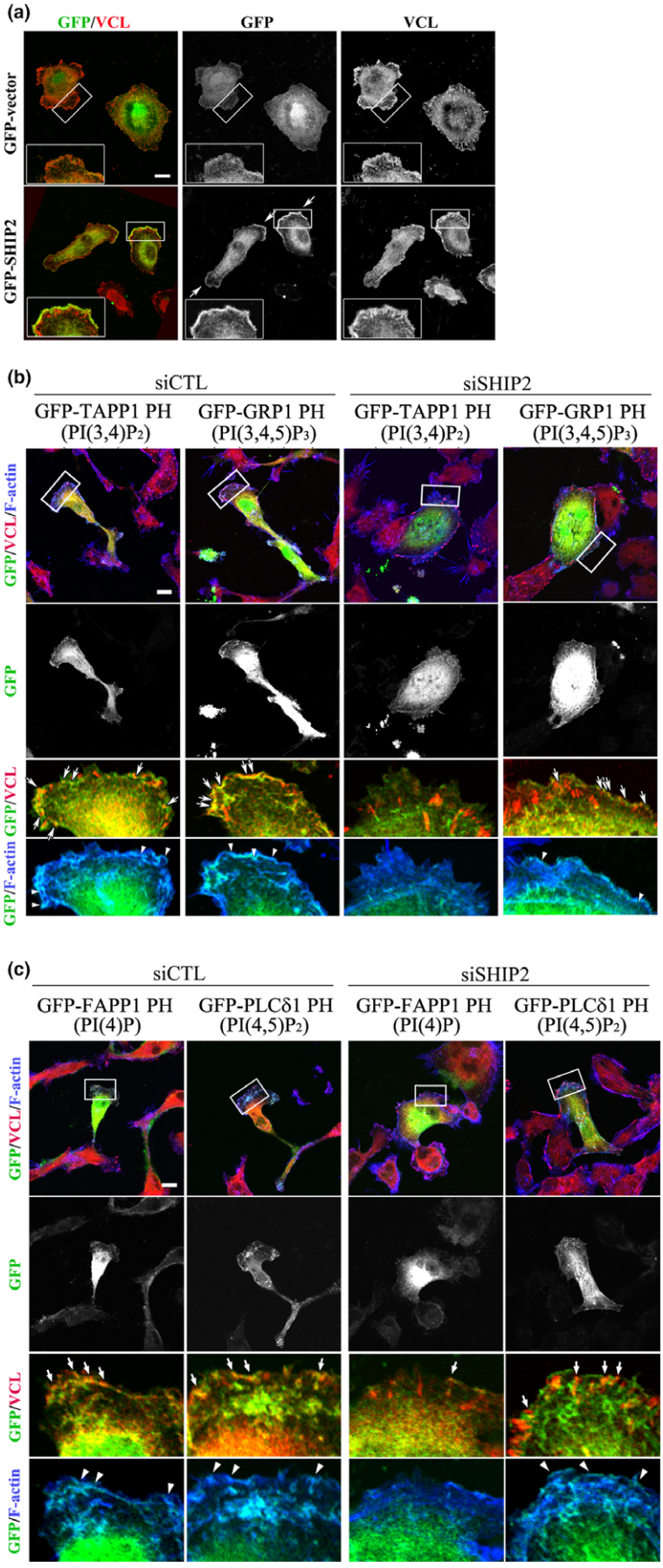

Fig. 2. Effect of SHIP2 knockdown on PIP_3 and PI(3,4)P_2 levels at the focal adhesions. (a) GFP-SHIP2-expressing MDA-MB-231 cells were stained with a VCL antibody. Enlarged images of the boxed areas are indicated in the lower panels. The arrows indicate membrane ruffles. Scale bar = 10 μm. (b) MDA-MB-231 cells transfected with control (siCTL) or SHIP2 #1 (siSHIP2) siRNA were stained with VCL. For the detection of PIP_3 and PI(3,4)P_2, GFP-GRP1-PH or GFP-TAPP1 PH was also expressed in these cells. F-actin was visualized with Alexa Fluor 647 labeled-phalloidin. Enlarged images of boxed areas are indicated in the lower panels. The arrows and arrowheads indicate focal adhesions and membrane ruffles, respectively. Scale bar = 10 μm. (c) MDA-MB-231 cells transfected with Control (siCTL) or SHIP2 #1 (siSHIP2) siRNA were stained with VCL. To detect PI(4,5)P_2 and PI(4)P, GFP-PLCδ1-PH or GFP-FAPP1 PH was also expressed in these cells. F-actin was visualized with Alexa Fluor 647 labeled-phalloidin. Enlarged images of boxed areas are indicated in the lower panels. The arrows and arrowheads indicate focal adhesions and membrane ruffles, respectively. Scale bar = 10 μm.

to the lamellipodia and VCL-positive focal contacts (Fig. 2a). Since focal contacts and lamellipodia are formed during the initial stages of cell spreading before the development of focal adhesions, these results imply a role of SHIP2 in the assembly and/or disassembly of focal contacts. Next, the localization of PIP_3 and $PI(3,4)P_2$ were observed using GFP-GRP1 PH and GFP-TAPP1 PH, which specifically bind to PIP_3 and $PI(3,4)P_2$, respectively.[50] PIP_3 was predominantly localized to the lamellipodia and focal contacts at the front of cells in both control- and SHIP2 siRNA-transfected cells (Fig. 2b). In addition, $PI(3,4)P_2$ was localized to the lamellipodia and partially to VCL-positive focal contacts. In SHIP2 knockdown cells, VCL-positive focal contacts were observed and $PI(3,4)P_2$ localization was no longer observed (Fig. 2b). Because SHIP2 also controls $PI(4,5)P_2$ and PI(4)P at the plasma membrane in 1321 N1 glioblastoma cells,[30] the effect of SHIP2 knockdown on these phosphoinositides at the plasma membrane was examined. Representative images of GFP-FAPP1 PH and GFP-PLCδ1 PH, which bind to PI(4)P and $PI(4,5)P_2$, are shown. Localization of these phosphoinositides at the PM was not changed by SHIP2 depletion in MDA-MB-231 cells (Fig. 2c). To examine the effect of PIP_3 generation on focal adhesion formation, MDA-MB-231 cells were treated with PI3-kinase inhibitors including wortmannin and LY294002. These compounds completely inhibited PIP_3-dependent Akt phosphorylation, showing complete abolishment of PIP_3 generation (Fig. 3a). These inhibitors increased PAX phosphorylation (Fig. 3a) and increased focal adhesions number and cell areas (Fig. 3b–d). To clarify whether $PI(3,4)P_2$ contributes to these changes, the effect of PI3-kinase inhibitors on relative amount of $PI(3,4)P_2$ and $PI(4,5)P_2$ levels at the PM were examined. Fluorescence intensity of EGFP-TAPP1 PH domain that binds to $PI(3,4)P_2$, has been measured to quantify $PI(3,4)P_2$ levels at the plasma membrane. We found that PM $PI(3,4)P_2$ levels were decreased, whereas the fluorescence intensity of EGFP-PLCδ1 PH that binds to $PI(4,5)P_2$ was not altered by these inhibitors (Fig. 3e,f). These results suggest that the generation of $PI(3,4)P_2$ by SHIP2 promotes the formation of lamellipodia and suppresses the development of focal adhesions, whereas PIP_3 and $PI(4,5)P_2$ are unlikely to play any role in these processes.

Differential effect of PTEN and SHIP2 knockdown on focal adhesion development and cell invasion. PTEN is a 3-phosphatase of PIP_3 and $PI(3,4)P_2$, which catalyzes the production of $PI(3,4)P_2$ and PI(4)P, respectively. We compared the effect of SHIP2 and PTEN knockdown on focal adhesions in MDA-MB-231 cells. SHIP2 knockdown did not alter Akt phosphorylation, whereas PTEN knockdown increased the levels of phosphorylated Akt (Fig. 4a). SHIP2 knockdown increased phosphorylated PAX, which was not increased by PTEN knockdown (Fig. 4a). PTEN silencing induced aberrant membrane ruffle formation and decreased cell area (Fig. 4b–d). Interestingly, the combination with SHIP2 knockdown suppressed these phenotypes (Fig. 4b–d). Compared to that in control cells, the fluorescence intensity of EGFP-TAPP1 PH was decreased by 60% in SHIP2-depleted cells, increased by 10% in PTEN-depleted cells, and decreased by 50% upon combined depletion of SHIP2 and PTEN (Fig. 4e). Fluorescence intensity of the EGFP-PLCδ1 PH was increased by 20% in SHIP2-depleted cells, and was not changed in PTEN-

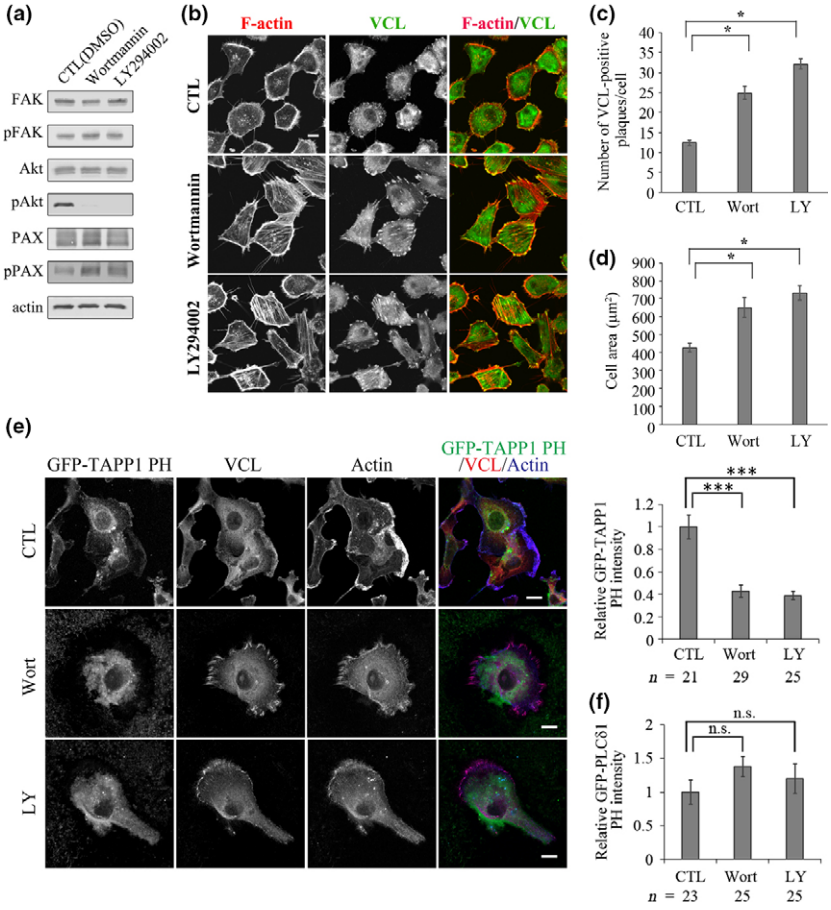

Fig. 3. Effect of PI3K inhibitors on focal adhesion formation and cell spreading. (a) Lysates from DMSO-, wortmannin-, or LY294002-treated MDA-MB-231 cells were subjected to western blot analysis using FAK, phospho-FAK, Akt, phospho-Akt, PAX, phospho-PAX, and actin antibodies. (b) Effect of PI3K inhibitors on focal adhesion formation. After treatment with DMSO (CTL), wortmannin, or LY294002, cells were fixed and stained with an anti-vinculin antibody. Actin was visualized by rhodamine-phalloidin. Scale bar = 10 μm. (c,d) Quantification of focal adhesions per cell (c) and measurement of cell area (d) from (b). Data represent the mean ± SD of 30 cells for CTL, wortmannin, and LY294002-treated cells, respectively. $*P < 0.05$. (e) Quantification of the relative amounts of $PI(3,4)P_2$ at the PM in MDA-MB-231 cells treated with PI3-kinase inhibitors. To detect $PI(3,4)P_2$, GFP-TAPP1 PH was expressed in these cells. Cells were stained with an anti-vinculin antibody. Actin was visualized by Alexa Fluor 647-conjugated phalloidin. Scale bar = 20 μm. Data represent the mean ± SD. *n*, no of analyzed cells pooled from three independent experiments. $***P < 0.001$. (f) Quantification of the relative amounts of $PI(4,5)P_2$ at the PM in MDA-MB-231 cells treated with PI3-kinase inhibitors. For the detection of $PI(4,5)P_2$, GFP-PLCδ1-PH was expressed in these cells. Data represent the mean ± SD. *n*, no. analyzed cells pooled from three independent experiments. n.s.: not significant.

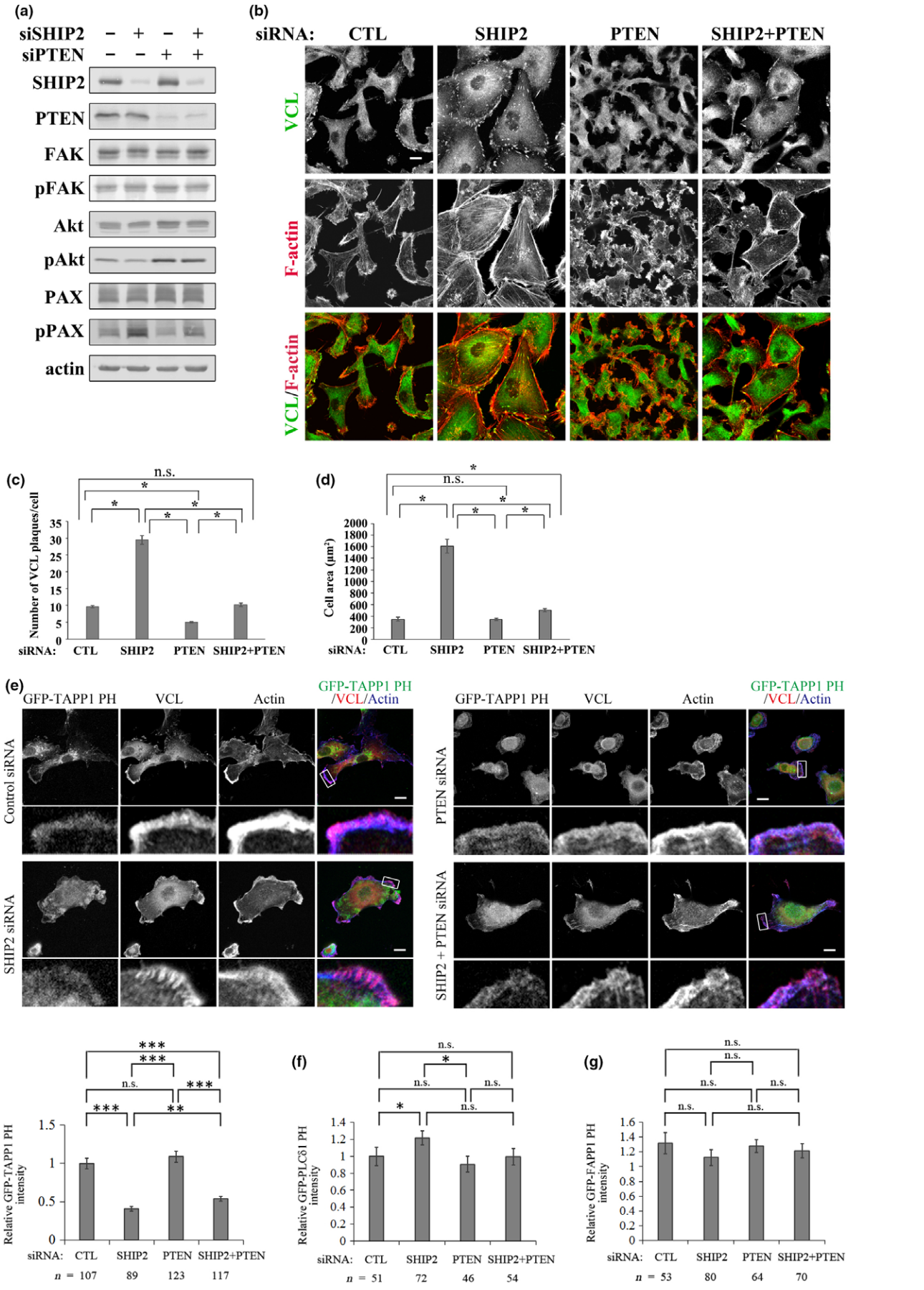

Fig. 4. Effect of SHIP2 and PTEN silencing on focal adhesion-related signaling molecules and focal adhesion formation. (a) Phosphorylation of PAX, FAK, and Akt in MDA-MB-231 cells transfected with PTEN siRNA and/or SHIP2 siRNA. Lysates were subjected to western blotting with the indicated antibodies. (b) PTEN and/or SHIP2-silenced MDA-MB-231 cells were stained with an anti-VCL antibody. Actin was visualized with rhodamine-phalloidin. Scale bar = 10 μm. (c) Quantification of focal adhesions per cell from (b). (d) Cell area of siRNA-transfected cells from (b). Data represent the mean ± SD of 30 cells for control siRNA, PTEN siRNA, siSHIP2, PTEN siRNA and SHIP2 siRNA, respectively. $*P < 0.05$. (e) Quantification of the relative amounts of $PI(3,4)P_2$ at the PM in MDA-MB-231 cells transfected with SHIP2 siRNA and PTEN siRNA. To detect $PI(3,4)P_2$, GFP-TAPP1 PH, was expressed in these cells. The representative images were shown and enlarged images of the boxed areas are indicated in the lower panels. Cells were stained with an anti-vinculin antibody. Actin was visualized with Alexa Fluor 647-conjugated-phalloidin. Scale bar = 20 μm. Data represent the mean ± SD. *n*, no. analyzed cells pooled from six independent experiments. $**P < 0.01$, $***P < 0.001$ (Student–Newman-Keuls multiple comparison tests). (f,g) Quantification of the relative amounts of $PI(4,5)P_2$ (f) and PI(4)P (g) at the PM in MDA-MB-231 cells transfected with PTEN siRNA and/or SHIP2 siRNA. For the detection of $PI(4,5)P_2$ and PI(4)P, GFP-PLCδ1-PH or GFP-FAPP1 PH was expressed in these cells. Data represent the mean ± SD. *n*, no. analyzed cells pooled from three independent experiments. $*P < 0.05$ (Student–Newman–Keuls multiple comparison tests), n.s.: not significant.

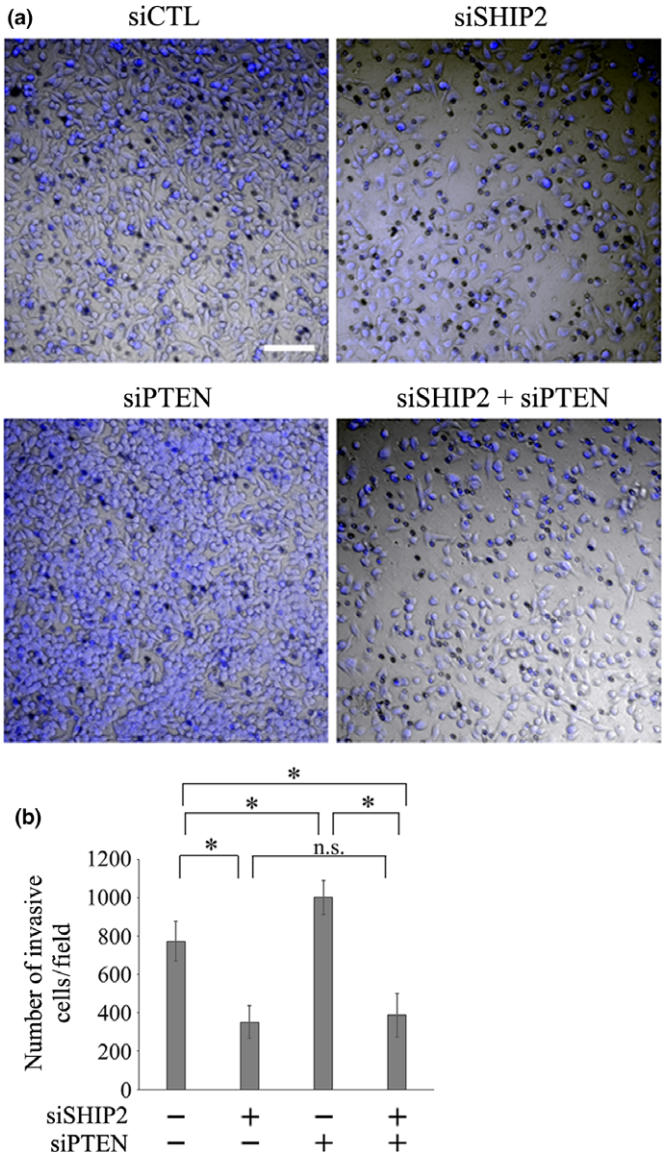

Fig. 5. Effect of SHIP2 and PTEN knockdown on cell invasion. (a) An invasion assay was performed using MDA-MB-231 cells. Cells transfected with PTEN siRNA and/or SHIP2 siRNA were seeded in Matrigel invasion chambers and allowed to invade the Matrigel for 22 h. Invading cells were fixed and stained with propidium iodide. Scale bar = 100 μm. (b) The number of invading cells, shown in (a), was counted. Results represent the mean ± SD of five independent experiments. $*P < 0.01$. n.s.: not significant.

depleted cells (Fig. 4f). Fluorescence intensities of EGFP-FAPP1 PH were not changed in SHIP2- or PTEN-depleted cells (Fig. 4g). These results suggest that $PI(3,4)P_2$ might play an important role in membrane ruffle and lamellipodia formation in MDA-MB-231 cells. Next, the effect of SHIP2 and/or PTEN knockdown on cell invasion in Matrigel was examined. SHIP2 silencing decreased the number of invasive cells, whereas PTEN-silencing increased this parameter (Fig. 5a,b). Interestingly, combined knockdown of SHIP2 and PTEN suppressed the invasion of MDA-MB-231 cells (Fig. 5a,b).

Lpd knockdown increases focal adhesion development. Lpd has a PH domain, which binds to $PI(3,4)P_2$, and plays a crucial role in membrane ruffle and lamellipodia formation through sequential activation of the Rac-WAVE pathway.[3,51] We thus examined changes in the formation of focal adhesions and lamellipodia after Lpd knockdown. Lpd knockdown slightly increased phospho-PAX (Fig. 6a), induced focal adhesion formation and cell spreading (Fig. 6b–d), and inhibited cell invasion in Matrigel (Fig. 6e,f). These results are very similar to those of SHIP2 knockdown, and suggest that the inhibition of the $PI(3,4)P_2$-dependent Lpd-Rac-WAVE signaling pathway causes a shift from membrane ruffling and lamellipodia formation to focal adhesion development.

$PI(3,4)P_2$ is required for lamellipodia formation. We hypothesized that overexpression of TAPP1 PH, which binds to $PI(3,4)P_2$, would efficiently suppress Lpd activation leading to lamellipodia formation. To clarify the importance of $PI(3,4)P_2$ in focal adhesion formation and cell spreading, we examined the effect of TAPP1 PH domain overexpression on these events. GFP-TAPP1 PH overexpression induced focal adhesion formation and cell spreading. However, the expression of GFP-GRP1 PH did not affect these parameters (Fig. 7a–c). These results show that $PI(3,4)P_2$ generation promotes cell membrane ruffling and lamellipodia formation, leading to cell invasion, whereas suppression of $PI(3,4)P_2$ production results in focal adhesion and stress fiber formation, leading to cell spreading and increased cell area.

Discussion

Alteration of PI3KCA, PTEN, PIP_3 5-phosphatases, and INPP4B are common events in breast cancer,[5,6] suggesting the importance of phosphoinositides in tumorigenesis. In this study, we revealed that $PI(3,4)P_2$, rather than PIP_3, is important for lamellipodia formation in human cancer cells, which leads to cell motility and invasion. In basal-breast cancer cell lines, and specifically MDA-MB-231 cells, which lack INPP4B, intracellular PIP_3 and $PI(3,4)P_2$ amounts are under the control of PTEN and PIP_3 phosphatases including SHIP2. SHIP2 expression is elevated in breast cancer cells promoting cell migration and tumor metastasis. The function of SHIP2 in glioblastoma cell migration has been previously evaluated.[30] SHIP2-depletion potentiated migration in PTEN-null 1321 N1 glioblastoma cells, whereas it reduced migration in PTEN-

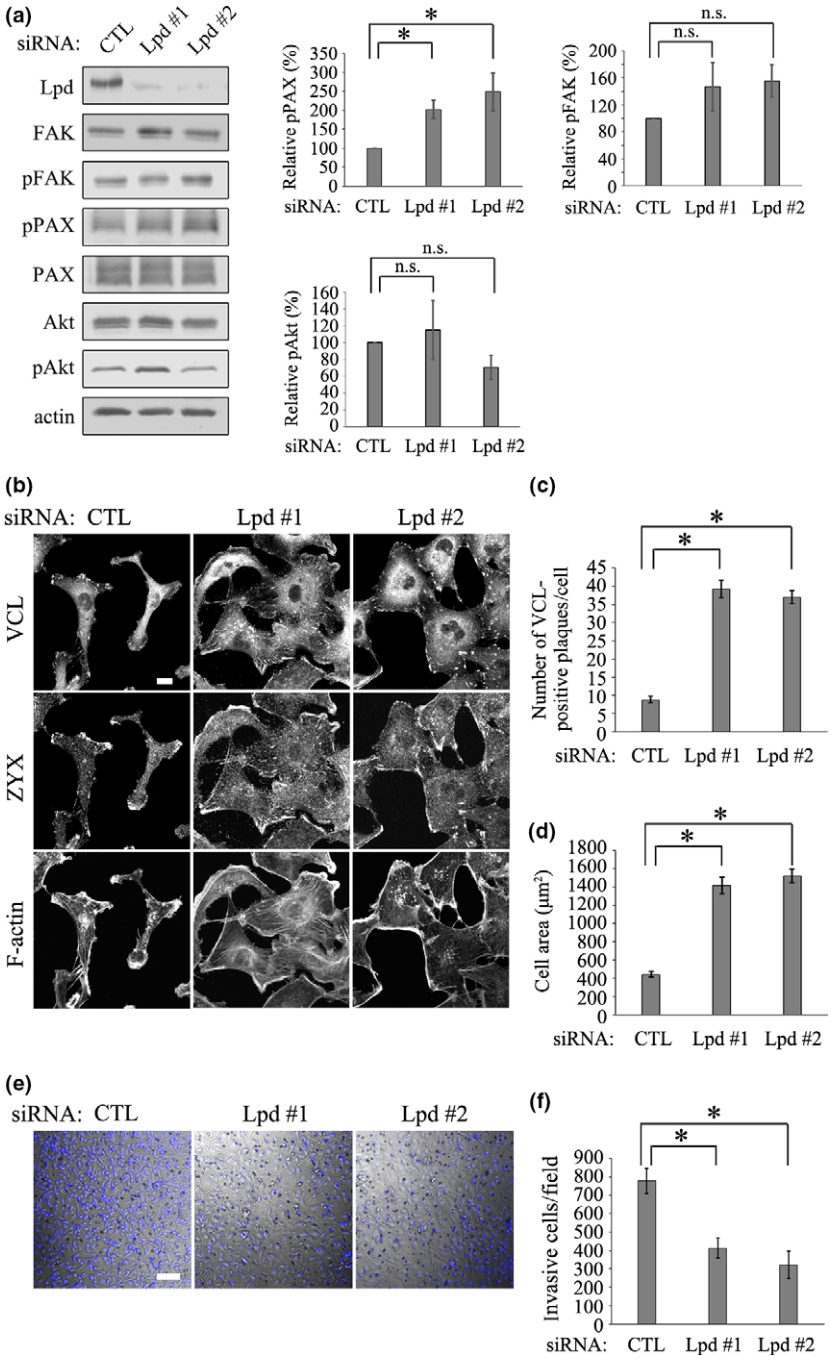

Fig. 6. Lpd knockdown results in focal adhesion formation. (a) Phosphorylation of PAX, FAK, and Akt in MDA-MB-231 cells transfected with control- (CTL) or Lpd-targeted siRNA. Lysates were subjected to western blot analyses with the indicated antibodies. Results are presented as the mean ± SD of three independent experiments. *$P < 0.01$, n.s.: not significant. (b) MDA-MB-231 cells transfected with control- (CTL) or Lpd-targeted siRNA were stained with anti-VCL and anti-ZYX antibodies. Actin was visualized by Alexa Fluor 647-conjugated phalloidin. Scale bar = 10 μm. (c,d) Quantification of focal adhesion number per cell (c) and measurement of cell area (d) from cells shown in (a). Data represent the mean ± SD of 35 cells for the control, siLpd #1, and siLpd #2, respectively. *$P < 0.01$. (e) An invasion assay was performed using MDA-MB-231 cells. Cells transfected with siLpd #1 or siLpd #2 were seeded in Matrigel invasion chambers and allowed to invade the Matrigel for 22 h. Invading cells were fixed and stained with propidium iodide. Scale bar = 100 μm. (f) The number of invading cells, shown in (e), was counted. Results represent the mean ± SD of three independent experiments. *$P < 0.01$.

containing LN229 cells.[30] These results are not consistent because SHIP2 functions as an oncogene. However, it also functions as a tumor suppressor in different cancer cells, which might be explained by different functions of PIP_3 and PI(3,4)P_2 in cancer cells. Therefore, it was suggested that the effect of SHIP2 on cell migration is dependent on cell types and is affected by PTEN status. Here, we show that in MDA-MB-231 breast cancer cells, SHIP2-depletion increased focal adhesion formation and cell area regardless of PTEN expression levels (Figs 4b–d), suggesting that PI(3,4)P_2 generated by SHIP2 acts on focal adhesion dynamics and cell invasion. Akt phosphorylation was not markedly increased by SHIP2 knockdown in contrast to PTEN knockdown, indicating that PIP_3 levels were not significantly affected by SHIP2. In contrast, knockdown of PTEN enhanced Akt phosphorylation markedly with slight increases in cell adhesion formation and cell invasion. These results suggest that PTEN knockdown increases PIP_3, and slightly increases PI(3,4)P_2 levels, in these cells. Treatment of PI 3-kinase inhibitors decreased PIP_3 and PI(3,4)P_2 generation, which in turn resulted in an increased number of focal adhesions and cell area. Taken together, PIP_3 and PI(3,4)P_2 have distinct roles in basal breast cancer phenotypes (Fig. 8). In MDA-MB-231 cells, which have high PTEN expression,[52] PTEN predominantly regulates PIP_3 levels, and is related to PI3-kinase signaling. In contrast, SHIP2 plays a role in the generation of PI(3,4)P_2, which in turn leads to Lpd

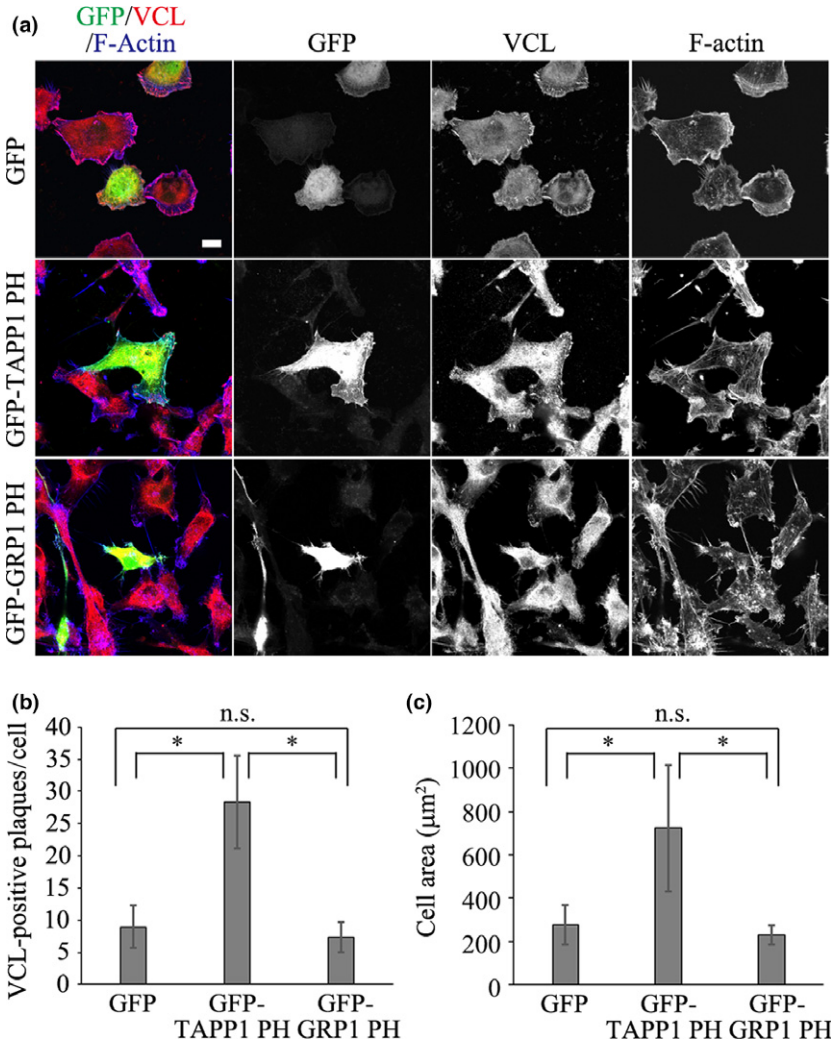

Fig. 7. Effect of phosphoinositide binding domain expression on focal adhesion formation. (a) Expression of GFP, GFP-TAPP1 PH, or GFP-GRP1 PH in MDA-MB-231 cells to mask $PI(3,4)P_2$ or PIP_3, respectively. The cells were stained with an anti-VCL antibody and actin was visualized with Alexa Fluor 647-labeled phalloidin. Scale bar = 10 μm. (b) Quantification of focal adhesions per cell from (a). (c) Cell area of cells from (a). Data represent the mean ± SD of 50 cells for control GFP, 27 cells for GFP-TAPP1 PH, and eight cells for GFP-GRP1 PH, respectively. $*P < 0.01$. n.s.: not significant.

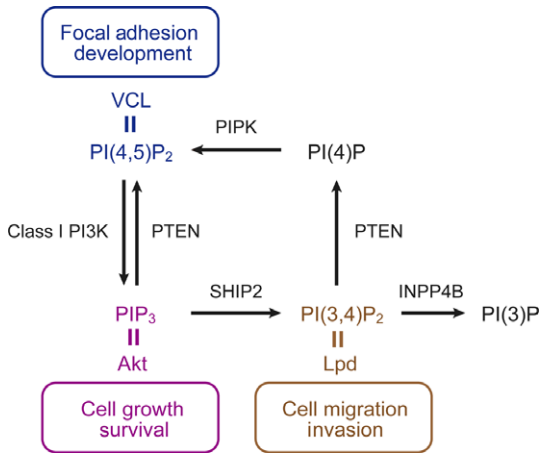

Fig. 8. Schematic representation of the distinct roles of $PI(3,4)P_2$, $PI(4,5)P_2$ and PIP_3 in focal adhesion formation and cell spreading in breast cancer cells. Examples of molecules known to be involved in phosphoinositide turnover and to function downstream of each phosphoinositide are shown.

signaling and lamellipodia formation. The control effect of SHIP2 on cell migration varies widely in different cell types. Although the reason for the differences between cells is not understood, differences in the status of other phosphoinositide phosphatases including INPP4B can affect the amounts of phosphoinositides including PIP_3, $PI(3,4)P_2$, and $PI(4,5)P_2$ and determine the function of SHIP2 in invasive phenotypes of cancer cells.

Among these phosphoinositides, $PI(4,5)P_2$ increases FAK phosphorylation and facilitates directional cell migration through interaction with its effector IQ Motif Containing GTPase Activating Protein 1 (IQGAP1).[53] In 1321 N1 glioblastoma cells, SHIP2 depletion increased $PI(4,5)P_2$ levels by two-fold and facilitated FAK phosphorylation. In MDA-MB-231 cells, SHIP2 depletion increased the amount of $PI(4,5)P_2$ by only 20%; and we could not detect an increase in FAK phosphorylation. These results suggest that SHIP2 does not affect $PI(4,5)P_2$-dependent regulation of cell migration and invasion in MDA-MB-231 cells. Lpd was shown to be required for metastasis in an orthotopic breast cancer mouse model, and increased Lpd expression suppressed metastasis-free survival in breast cancer patients.[51] These data suggest that the inhibition of Lpd-Rac-WAVE pathway causes a shift from membrane ruffling and lamellipodia formation to focal adhesion development. Although underlying mechanisms of how $PI(3,4)P_2$ and its downstream effectors mediate PAX phosphorylation remain to be solved, increase in PAX phosphorylation by SHIP2 and Lpd knockdown is likely to induce development of

focal adhesion and enlargement of breast cancer cell. Thus, it is possible that SHIP2 enhances the formation of PI(3,4)P_2, which in turn activates Lpd, leading to increased cell invasion and metastasis.

Author contribution

M. F and T. I. performed the experiments and analyzed the data. T. I and T. T designed the study and wrote the paper. All authors discussed the results and commented on the manuscript.

Acknowledgments

We are grateful to Shunichi Nakamura (Kobe University Graduate School of Medicine) for their assistance. This work was supported by grants to T. I. from the Japan Society for the Promotion of Science (JSPS; Kakenhi grant number 16K08585). The funding agency had no role in the study design, data collection and analysis, decision to publish, or presentation of the manuscript.

Disclosure

The authors have no conflict of interest.

References

1 Krause M, Gautreau A. Steering cell migration: lamellipodium dynamics and the regulation of directional persistence. *Nat Rev Mol Cell Biol* 2014; **15**: 577–90.
2 Bae YH, Ding Z, Das T, Wells A, Gertler F, Roy P. Profilin1 regulates PI (3,4)P2 and lamellipodin accumulation at the leading edge thus influencing motility of MDA-MB-231 cells. *Proc Natl Acad Sci USA* 2010; **107**: 21547–52.
3 Law AL, Vehlow A, Kotini M *et al.* Lamellipodin and the Scar/WAVE complex cooperate to promote cell migration in vivo. *J Cell Biol* 2013; **203**: 673–89.
4 Lopez-Knowles E, O'Toole SA, McNeil CM *et al.* PI3K pathway activation in breast cancer is associated with the basal-like phenotype and cancer-specific mortality. *Int J Cancer* 2010; **126**: 1121–31.
5 Ma CX, Ellis MJ. The Cancer Genome Atlas: clinical applications for breast cancer. *Oncology (Williston Park)* 2013; **27**(1263–9): 74–9.
6 Pang B, Cheng S, Sun SP *et al.* Prognostic role of PIK3CA mutations and their association with hormone receptor expression in breast cancer: a meta-analysis. *Sci Rep* 2014; **4**: 6255.
7 Cuorvo LV, Verderio P, Ciniselli CM *et al.* PI3KCA mutation status is of limited prognostic relevance in ER-positive breast cancer patients treated with hormone therapy. *Virchows Arch* 2014; **464**: 85–93.
8 Gonzalez-Angulo AM, Chen H, Karuturi MS *et al.* Frequency of mesenchymal-epithelial transition factor gene (MET) and the catalytic subunit of phosphoinositide-3-kinase (PIK3CA) copy number elevation and correlation with outcome in patients with early stage breast cancer. *Cancer* 2013; **119**: 7–15.
9 Stemke-Hale K, Gonzalez-Angulo AM, Lluch A *et al.* An integrative genomic and proteomic analysis of PIK3CA, PTEN, and AKT mutations in breast cancer. *Can Res* 2008; **68**: 6084–91.
10 Maehama T, Dixon JE. The tumor suppressor, PTEN/MMAC1, dephosphorylates the lipid second messenger, phosphatidylinositol 3,4,5-trisphosphate. *J Biol Chem* 1998; **273**: 13375–8.
11 Stambolic V, Suzuki A, de la Pompa JL *et al.* Negative regulation of PKB/Akt-dependent cell survival by the tumor suppressor PTEN. *Cell* 1998; **95**: 29–39.
12 Liu P, Cheng H, Roberts TM, Zhao JJ. Targeting the phosphoinositide 3-kinase pathway in cancer. *Nat Rev Drug Discovery* 2009; **8**: 627–44.
13 Li J, Yen C, Liaw D *et al.* PTEN, a putative protein tyrosine phosphatase gene mutated in human brain, breast, and prostate cancer. *Science* 1997; **275**: 1943–7.
14 Steck PA, Pershouse MA, Jasser SA *et al.* Identification of a candidate tumour suppressor gene, MMAC1, at chromosome 10q23.3 that is mutated in multiple advanced cancers. *Nat Genet* 1997; **15**: 356–62.
15 Liaw D, Marsh DJ, Li J *et al.* Germline mutations of the PTEN gene in Cowden disease, an inherited breast and thyroid cancer syndrome. *Nat Genet* 1997; **16**: 64–7.
16 Rhei E, Kang L, Bogomolniy F, Federici MG, Borgen PI, Boyd J. Mutation analysis of the putative tumor suppressor gene PTEN/MMAC1 in primary breast carcinomas. *Can Res* 1997; **57**: 3657–9.
17 Fedele CG, Ooms LM, Ho M *et al.* Inositol polyphosphate 4-phosphatase II regulates PI3K/Akt signaling and is lost in human basal-like breast cancers. *Proc Natl Acad Sci USA* 2010; **107**: 22231–6.
18 Gewinner C, Wang ZC, Richardson A *et al.* Evidence that inositol polyphosphate 4-phosphatase type II is a tumor suppressor that inhibits PI3K signaling. *Cancer Cell* 2009; **16**: 115–25.
19 Bredel M, Bredel C, Juric D *et al.* High-resolution genome-wide mapping of genetic alterations in human glial brain tumors. *Can Res* 2005; **65**: 4088–96.
20 Liang Y, Diehn M, Watson N *et al.* Gene expression profiling reveals molecularly and clinically distinct subtypes of glioblastoma multiforme. *Proc Natl Acad Sci USA* 2005; **102**: 5814–9.
21 Saxena A, Clark WC, Robertson JT, Ikejiri B, Oldfield EH, Ali IU. Evidence for the involvement of a potential second tumor suppressor gene on chromosome 17 distinct from p53 in malignant astrocytomas. *Can Res* 1992; **52**: 6716–21.
22 Davies EM, Kong AM, Tan A *et al.* Differential SKIP expression in PTEN-deficient glioblastoma regulates cellular proliferation and migration. *Oncogene* 2015; **34**: 3711–27.
23 Ooms LM, Binge LC, Davies EM *et al.* The Inositol Polyphosphate 5-Phosphatase PIPP Regulates AKT1-dependent breast cancer growth and metastasis. *Cancer Cell* 2015; **28**: 155–69.
24 Giuriato S, Blero D, Robaye B, Bruyns C, Payrastre B, Erneux C. SHIP2 overexpression strongly reduces the proliferation rate of K562 erythroleukemia cell line. *Biochem Biophys Res Commun* 2002; **296**: 106–10.
25 Taylor V, Wong M, Brandts C *et al.* 5' phospholipid phosphatase SHIP-2 causes protein kinase B inactivation and cell cycle arrest in glioblastoma cells. *Mol Cell Biol* 2000; **20**: 6860–71.
26 Clement S, Krause U, Desmedt F *et al.* The lipid phosphatase SHIP2 controls insulin sensitivity. *Nature* 2001; **409**: 92–7.
27 Prasad N, Topping RS, Decker SJ. Src family tyrosine kinases regulate adhesion-dependent tyrosine phosphorylation of 5'-inositol phosphatase SHIP2 during cell attachment and spreading on collagen I. *J Cell Sci* 2002; **115**: 3807–15.
28 Takabayashi T, Xie MJ, Takeuchi S *et al.* LL5beta directs the translocation of filamin A and SHIP2 to sites of phosphatidylinositol 3,4,5-triphosphate (PtdIns(3,4,5)P3) accumulation, and PtdIns(3,4,5)P3 localization is mutually modified by co-recruited SHIP2. *J Biol Chem* 2010; **285**: 16155–65.
29 Edimo WE, Ramos AR, Ghosh S, Vanderwinden JM, Erneux C. The SHIP2 interactor Myo1c is required for cell migration in 1321 N1 glioblastoma cells. *Biochem Biophys Res Commun*. 2016; **576**: 508–14.
30 Edimo WE, Ghosh S, Derua R *et al.* SHIP2 controls plasma membrane PI (4,5)P2 thereby participating in the control of cell migration in 1321 N1 glioblastoma. *J Cell Sci* 2016; **129**: 1101–14.
31 Fu M, Fan W, Pu X *et al.* Elevated expression of SHIP2 correlates with poor prognosis in non-small cell lung cancer. *Int J Clin Exp Pathol* 2013; **6**: 2185–91.
32 Fu M, Gu X, Ni H *et al.* High expression of inositol polyphosphate phosphatase-like 1 associates with unfavorable survival in hepatocellular carcinoma. *Int J Clin Exp Pathol* 2013; **6**: 2515–22.
33 Yang J, Fu M, Ding Y *et al.* High SHIP2 expression indicates poor survival in colorectal cancer. *Dis Markers* 2014; **2014**: 218968.
34 Hasegawa J, Tokuda E, Tenno T *et al.* SH3YL1 regulates dorsal ruffle formation by a novel phosphoinositide-binding domain. *J Cell Biol* 2011; **193**: 901–16.
35 Sharma VP, Eddy R, Entenberg D, Kai M, Gertler FB, Condeelis J. Tks5 and SHIP2 regulate invadopodium maturation, but not initiation, in breast carcinoma cells. *Curr Biol* 2013; **23**: 2079–89.
36 Li H, Wu X, Hou S *et al.* Phosphatidylinositol-3,4-bisphosphate and its binding protein lamellipodin regulate chemotaxis of malignant B lymphocytes. *J Immunol* 2016; **196**: 586–95.
37 Hawkins PT, Stephens LR. Emerging evidence of signalling roles for PI(3,4) P2 in Class I and II PI3K-regulated pathways. *Biochem Soc Trans* 2016; **44**: 307–14.
38 Chen XJ, Squarr AJ, Stephan R *et al.* Ena/VASP proteins cooperate with the WAVE complex to regulate the actin cytoskeleton. *Dev Cell* 2014; **30**: 569–84.
39 Hansen SD, Mullins RD. Lamellipodin promotes actin assembly by clustering Ena/VASP proteins and tethering them to actin filaments. *eLife*. 2015. doi: 10, 7554/eLife.06585
40 Chen CS, Alonso JL, Ostuni E, Whitesides GM, Ingber DE. Cell shape provides global control of focal adhesion assembly. *Biochem Biophys Res Commun* 2003; **307**: 355–61.

41 Kanchanawong P, Shtengel G, Pasapera AM *et al.* Nanoscale architecture of integrin-based cell adhesions. *Nature* 2010; **468**: 580–4.
42 Bae YH, Mui KL, Hsu BY *et al.* A FAK-Cas-Rac-lamellipodin signaling module transduces extracellular matrix stiffness into mechanosensitive cell cycling. *Science Signaling* 2014; **7**: ra57.
43 Yamashita H, Ichikawa T, Matsuyama D *et al.* The role of the interaction of the vinculin proline-rich linker region with vinexin alpha in sensing the stiffness of the extracellular matrix. *J Cell Sci* 2014; **127**: 1875–86.
44 Furutani M, Itoh T, Ijuin T, Tsujita K, Takenawa T. Thin layer chromatography-blotting, a novel method for the detection of phosphoinositides. *J Biochem* 2006; **139**: 663–70.
45 Basson MD. An intracellular signal pathway that regulates cancer cell adhesion in response to extracellular forces. *Cancer Res* 2008; **68**: 2–4.
46 Calderwood DA, Shattil SJ, Ginsberg MH. Integrins and actin filaments: reciprocal regulation of cell adhesion and signaling. *J Biol Chem* 2000; **275**: 22607–10.
47 Parsons JT, Martin KH, Slack JK, Taylor JM, Weed SA. Focal adhesion kinase: a regulator of focal adhesion dynamics and cell movement. *Oncogene* 2000; **19**: 5606–13.
48 Burridge K, Turner CE, Romer LH. Tyrosine phosphorylation of paxillin and pp125FAK accompanies cell adhesion to extracellular matrix: a role in cytoskeletal assembly. *J Cell Biol* 1992; **119**: 893–903.
49 Wang SY, Basson MD. Akt directly regulates focal adhesion kinase through association and serine phosphorylation: implication for pressure-induced colon cancer metastasis. *Am J Physiol-Cell Ph* 2011; **300**: C657–70.
50 Dowler S, Currie RA, Campbell DG *et al.* Identification of pleckstrin-homology-domain-containing proteins with novel phosphoinositide-binding specificities. *Biochem J* 2000; **351**: 19–31.
51 Carmona G, Perera U, Gillett C *et al.* Lamellipodin promotes invasive 3D cancer cell migration via regulated interactions with Ena/VASP and SCAR/WAVE. *Oncogene*. 2016; **35**: 5155–69.
52 Sosa MS, Lopez-Haber C, Yang C *et al.* Identification of the Rac-GEF P-Rex1 as an essential mediator of ErbB signaling in breast cancer. *Mol Cell* 2010; **40**: 877–92.
53 Choi S, Thapa N, Hedman AC, Li Z, Sacks DB, Anderson RA. IQGAP1 is a novel phosphatidylinositol 4,5 bisphosphate effector in regulation of directional cell migration. *EMBO J* 2013; **32**: 2617–30.